Available online at www.sciencedirect.com

SciVerse ScienceDirect

Ceramics International 39 (2013) 1519–1523

CERAMICS INTERNATIONAL

www.elsevier.com/locate/ceramint

Synthesis and characterisation of thin-film TiO_2 dye-sensitised solar cell

M.S. Liang[a,*], C.C. Khaw[a], C.C. Liu[a], S.P. Chin[a], J. Wang[b], H. Li[b]

[a] *Department of Mechanical and Materials Engineering, Faculty of Engineering and Science, Universiti Tunku Abdul Rahman, 53300, Malaysia*
[b] *Department of Materials Science and Engineering, National University of Singapore, 117574, Singapore*

Received 24 April 2012; received in revised form 27 July 2012; accepted 27 July 2012
Available online 4 August 2012

Abstract

A TiO_2 dye-sensitised solar cell (DSSC) is fabricated and characterised using: X-ray diffraction (XRD) analysis, scanning electron microscopy (SEM), electron diffraction X-ray (EDX) analysis, UV–vis spectrometry and a current – voltage ($I-V$) test. Thicker anatase TiO_2 gives rise to better crystallinity and subsequently leads to better cell efficiency. Mesoporous TiO_2 with a suitable, average pore size results in higher conversion efficiency. Smaller particle sizes lead to higher dye uptake and increase short circuit current density, J_{sc}. Addition of scattering layer and/or dual $TiCl_4$ treatment for DSSCs having optimum thickness enhanced their performance. A DSSC having double TiO_2 layers (20 nm + 50 nm) with dual $TiCl_4$ treatment achieved the highest conversion efficiency of 9.78%.

Keywords: B. Electron microscopy; B. X-ray methods; D. TiO_2; Dye-sensitised solar cell

1. Introduction

The recent rising demand for and the escalating prices of fossil fuel and the environmental pollution resulting from conventional power generation has pushed the frontiers of science in looking for an alternative low-cost, clean and sustainable form of energy generation. Solar cell technology offers one of the promising sustainable energy sources for clean power generation. Dye-sensitised solar cells are the most intensely researched form of renewable energy due to the ease and low cost of fabrication [1–3]. In general, a dye-sensitised solar cell consists of four components, which are: the photo-electrode, counter electrode, sensitiser and electrolyte. The photo-electrode serves as a current collector whilst the counter electrode functions as a catalyst. The sensitiser is used to absorb light and the electrolyte containing the iodide/ tri-iodide redox couple provides electrons for the regeneration of oxidised sensitiser. Currently, efficiency of power conversion as high as 11% has been reported [4–5].

In this study, we synthesised DSSCs with different combinations of TiO_2 layers and employed various characterisation techniques to study those factors affecting or improving the conversion efficiency of the DSSCs.

2. Experimental

2.1. Materials and fabrication

Fluorine-doped tin oxide (FTO) glass substrate was washed with water and a mild detergent and dried by dryer. The cleaned FTO glass substrate was dipped in distilled water, acetone, absolute ethanol and deionised water and then heated at 400 °C to remove contaminants.

The titanium oxide (TiO_2) paste was deposited on the FTO coated glass substrate by doctor blade technique and sintered at a temperature of 455 °C. Three different types of paste with specific formulations were used. After cooling to 80 °C, the electrode was soaked in N719 dye solution and kept at room temperature for 24 h to ensure complete sensitiser uptake.

Meanwhile, a hole was drilled in the glass substrate printed with a platinum, Pt-based catalyst. The perforated glass substrate printed with Pt-based catalyst was dipped in absolute ethanol and deionised water and then heated at 400 °C for 15 min to remove contaminants.

---

[*] Corresponding author. Tel.: +60 341079802; fax: +60 341079803.
E-mail address: liangms@utar.edu.my (M.S. Liang).

0272-8842/$ - see front matter © 2012 Elsevier Ltd and Techna Group S.r.l. All rights reserved.
http://dx.doi.org/10.1016/j.ceramint.2012.07.099

The photo-electrode and counter electrode were assembled into a sandwich-type cell and sealed using a thermoplastic ionomer as a sealant, at 140 °C for 5 min. The electrolyte was introduced into the cell through vacuum backfilling. A drop of electrolyte was applied to the hole in the counter electrode. The air inside the cell was removed by using a small vacuum pump and the cell was then exposed to ambient pressure causing the electrolyte to be driven into the cell. Lastly, the hole was sealed using the thermoplastic sealant and a covering glass.

2.2. Titanium tetrachloride, $TiCl_4$ treatment

Dual titanium tetrachloride ($TiCl_4$) treatment was used in this research. The first treatment was performed prior to paste deposition, while the second treatment was performed after paste deposition.

A 50 mM aqueous $TiCl_4$ solution was prepared by diluting $TiCl_4$ with distilled water at room temperature. The FTO coated glass substrate was immersed in the 50 mM aqueous $TiCl_4$ solution at 70 °C for 30 min and then washed with ethanol and deionised water and placed in a dryer.

After the first treatment, TiO_2 paste was deposited on the FTO glass substrate. A second treatment was performed after the paste application by following the same procedure as the first. Then the electrode was sintered at 455 °C for 30 min. After cooling to 80 °C, the TiO_2 electrode was immersed into N719 dye solution for 24 h.

2.3. Measurements

The characteristics of the TiO_2 film may affect the dye adsorption and consequently influence the performance of the solar cell. Scanning electron microscopy (SEM) and electron diffraction X-ray (EDX) analysis were used to investigate the morphologies, particle and pore sizes and weight ratios of elements for the TiO_2 films. X-ray diffraction (XRD) techniques were employed to investigate the influence of thickness on the crystallinity of the TiO_2 film. UV–vis spectrometry was utilised to investigate dye loading. An $I-V$ test was used to determine the cell parameters, such as: short circuit current density, J_{sc}, open circuit voltage, V_{oc}, maximum power, P_{max} and conversion efficiency, η of the DSSCs.

3. Results and discussion

3.1. XRD

The XRD patterns of the TiO_2 films are shown in Fig. 1. The crystal structure of all TiO_2 films exhibit anatase phase as compared with ICDD 78-2486. Anatase phase appears as pyramid-like crystals, which have a higher surface area than rutile and brookite for optimum dye adsorption. Anatase has been the main subject of study in DSSCs because it is the primary crystal formed in the usual colloidal preparation method of the nanocrystalline TiO_2 electrode. Studies have revealed that DSSCs with pure rutile structure exhibited 30% smaller J_{sc} than pure anatase [6–7]. Crystallinity, as determined by XRD, increases with the increase of TiO_2 film thickness; better crystallinity leads to sharper peaks as shown in Fig. 1.

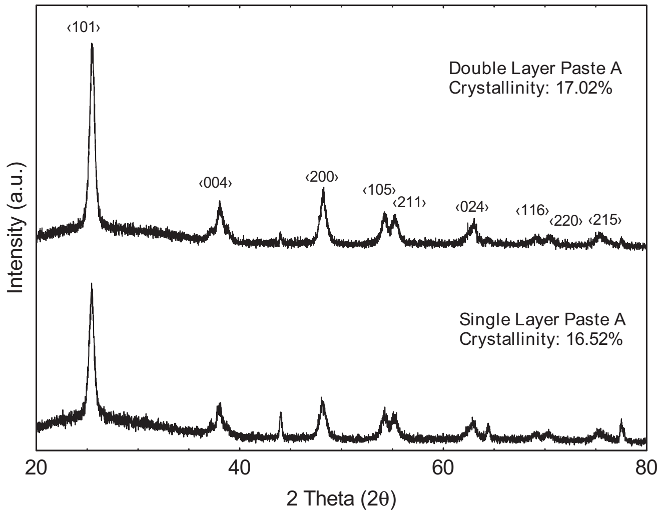

Fig. 1. XRD patterns of TiO_2 films for Paste A.

Table 1
Measured particle sizes and ideal sintered layer thicknesses of the three pastes.

Paste	Average particle sizes (nm)	Sintered layer (μm)	Type of layer
A	20–30	6–7	Active
B	50–60	7–8	Active
C	150–250	3	Scattering layer

3.2. SEM and EDX

Table 1 shows the measured particle sizes using SEM and the ideal sintered layer thickness of TiO_2. The average particle sizes for the two active layers (A and B) are 20–30 nm and 50–60 nm, respectively, whereas that of scattering layer C is 150–250 nm. The thicknesses for each sintered layer of paste A, B and C, are given as approximately 6–7 μm, 7–8 μm and 3 μm, respectively. Fig. 2 displays the micrographs and the weight ratios of the elements (determined by EDX) in the TiO_2 particles; approximately 62 wt% of titanium, 36 wt% of oxygen and minor traces of carbon. The presence of the carbon element can probably be attributed to the carbon tape used to anchor the sample to the holder and serves as an electron collector.

Fig. 3 shows the cross-section SEM image of the TiO_2 films: (a) mono-layer of Paste A, (b) double-layer of Paste B (c) double-layer Paste A with scattering layer (Paste C). The thicknesses of TiO_2 films measured from the cross-section are 5.47 μm, 19.0 μm, and 22.1 μm, respectively.

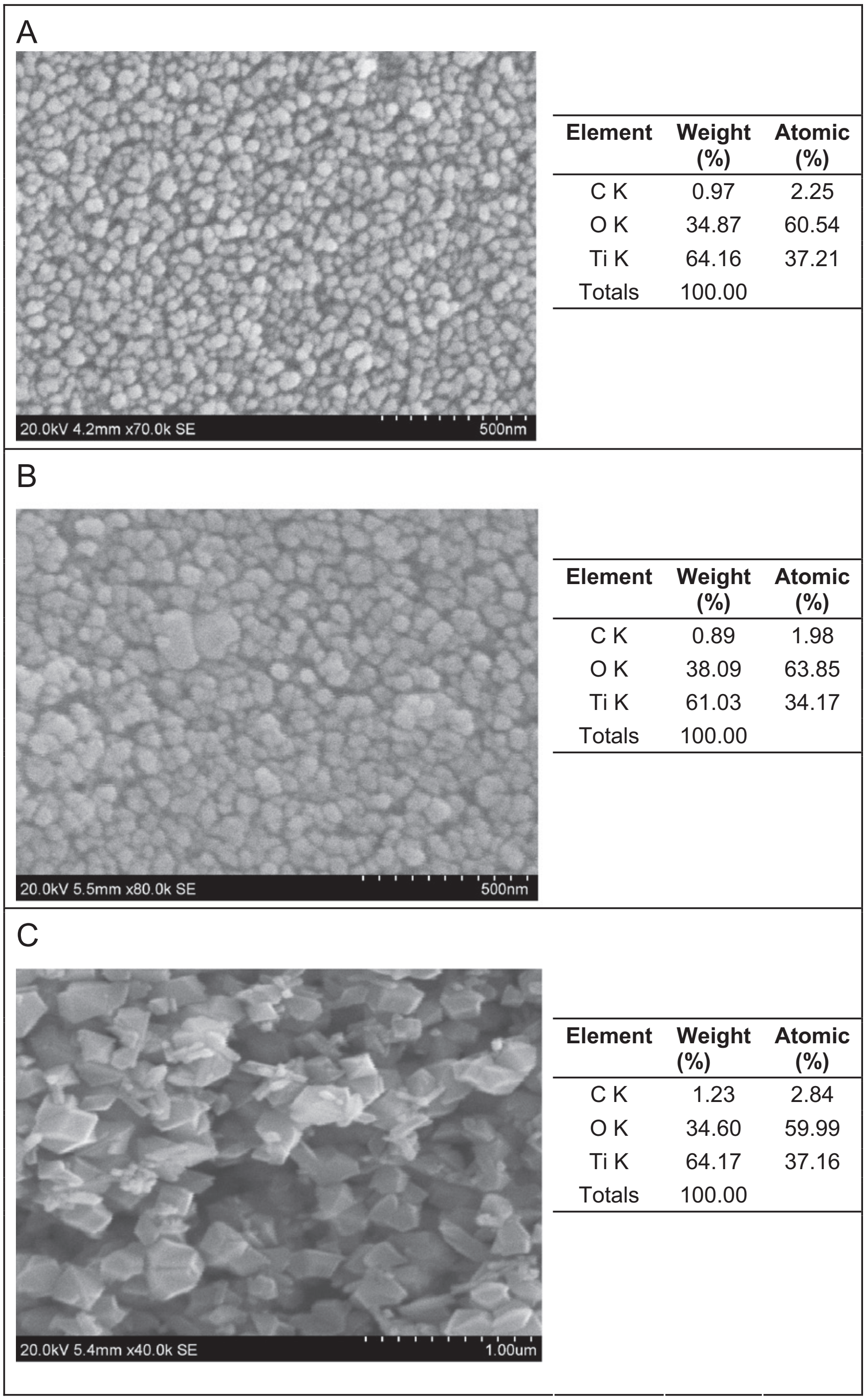

A

Element	Weight (%)	Atomic (%)
C K	0.97	2.25
O K	34.87	60.54
Ti K	64.16	37.21
Totals	100.00	

B

Element	Weight (%)	Atomic (%)
C K	0.89	1.98
O K	38.09	63.85
Ti K	61.03	34.17
Totals	100.00	

C

Element	Weight (%)	Atomic (%)
C K	1.23	2.84
O K	34.60	59.99
Ti K	64.17	37.16
Totals	100.00	

Fig. 2. SEM micrographs and EDX analysis of Paste A, B and C.

This shows that the doctor-blade method used in this project is able to produce a compatible sintered layer thickness, as specified in the formulation (Table 1). Therefore, it gives us confidence in the *I*–*V* measurements in a later section.

3.3. *UV–visible spectroscopy*

N719 dye is a hydrophilic dye that is soluble in alkaline water solutions. In this study, the sample for the UV–vis test was prepared by diluting the TiO_2 in a solution of sodium hydroxide, NaOH and ethanol.

Based on UV–vis spectroscopy, the absorption peaks of the N719 dye are at 309 nm, 368 nm and 509 nm. The peak around 509 nm shifts towards longer wavelengths as the concentration of the N719 dye is increased. This implies that the intermolecular interaction between the dye molecules affected the peak position in the visible portion [8].

Fig. 4 shows that the double layer photo-electrode with smaller particle size (e.g., Double layer Paste A), has a

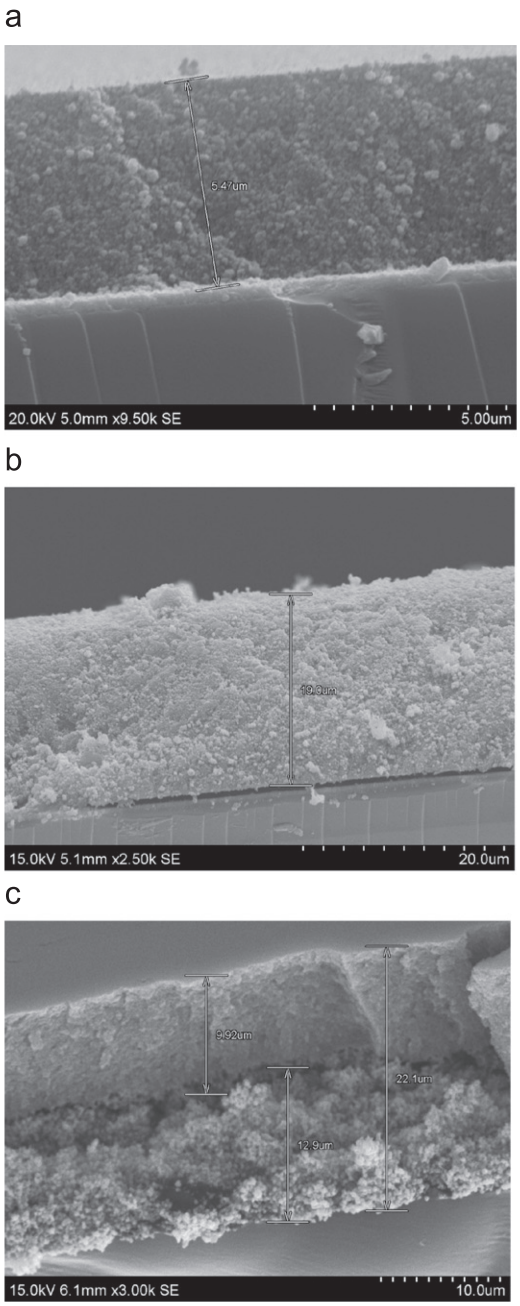

Fig. 3. Cross-section of the TiO_2 films (a) mono-layer of Paste A, (b) double-layer of Paste B and (c) double-layer Paste A with scattering layer (Paste C).

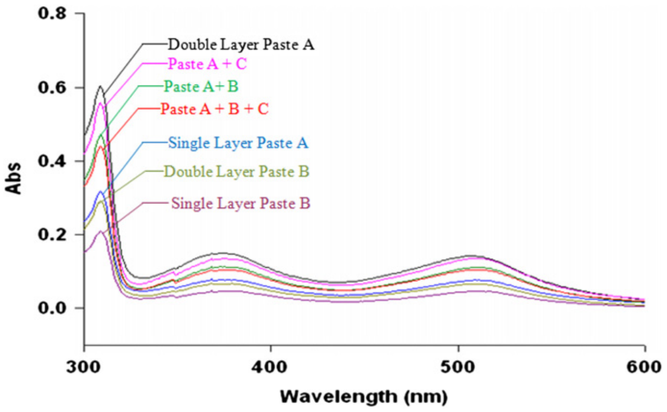

Fig. 4. UV–visible Spectrum for various samples.

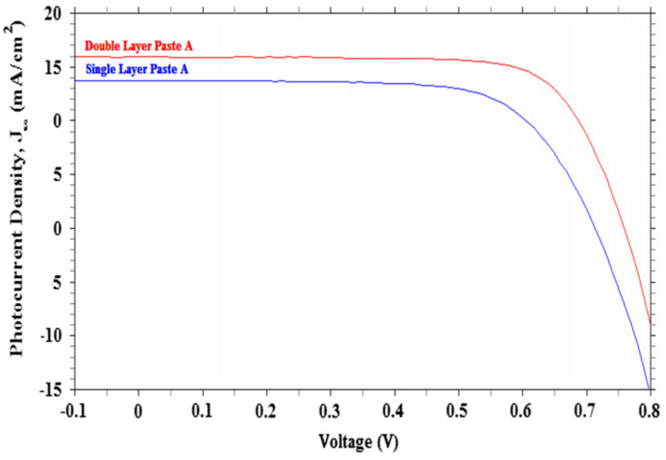

Fig. 5. Current–Voltage curve of Paste A.

Table 2
I–V test results and the layer thicknesses for different TiO_2 thin films.

Paste	J_{sc} (mA/cm^2)	*FF*	η (%)	t (μm)
Single layer Paste A	13.74	68.24	6.68	5.47
Single layer Paste B	14.63	66.55	6.73	7.61
Paste B+C	14.51	68.25	7.12	10.73
Double layer Paste A	15.93	73.34	8.86	12.50
Paste A+C	15.66	70.74	8.03	15.00
Paste A+B	16.30	72.01	9.16	14.70
Double layer Paste B	14.51	67.95	6.97	19.00
Paste A+B+C	16.21	70.00	8.42	20.1

higher dye loading than that of the larger particle size (e.g., Double layer Paste B); particle size and optimum TiO_2 thickness (12–14 μm) [9] are shown to affect dye loading. Higher dye loading is one of the factors that will lead to higher efficiency, as described in Section 3.4.

3.4. *I–V* Test

Fig. 5 shows that short circuit current density, J_{sc} increases with thicker TiO_2 film due to improvements in the ability of dye absorption as a result of the larger surface area of the TiO_2 particles. Improvements in J_{sc} will lead to an increase in the conversion efficiency, as shown in equation [10], $\eta=(V_{oc}\times J_{sc}\times FF)/P_{in}$, where *FF* is the fill factor, J_{sc} is the short circuit current, V_{oc} is the open circuit voltage and P_{in} is the incident light power intensity.

Within the optimum thickness range of the TiO_2 layer, a thicker layer will yield higher efficiency, as shown in Table 2. For example, double layer Paste A shows a reading of 8.86% compared with single layer Paste A at 6.68%. If double layer Paste B is within the optimum

Table 3
Effect of $TiCl_4$ treatment on solar efficiency.

Paste (without $TiCl_4$)	**without $TiCl_4$ η (%)**	**with $TiCl_4$ η (%)**
Double layer Paste A	8.86	9.15
Paste A+B	9.16	9.78
Double layer Paste A+C	8.03	8.90

Table 4
TiO_2 pore size.

Paste	Pore size (nm)
A	4–5
B	5–6

thickness range, it is expected to achieve much higher conversion efficiency, comparable to that of double layer Paste A (~9%). However, double layer Paste B only records a conversion efficiency of 6.97%, which is much lower than the expected result of ~9%, possibly due to cracks on the surface of the thicker film. Thick TiO_2 film tends to crack owing to shrinkage of the film during the removal of organic solvents [11]. This reduces electron transport efficiency and causes higher rates of recombination, thus lowering performance of the dye sensitised solar cell. The conversion efficiency of photo-electrodes with a single layer Paste B is improved when a scattering layer is added. This scattering layer increases the optical path length of incident photons resulting in higher interaction between photons and the sensitiser. However, the optimum thickness of paste must be taken into consideration; the conversion efficiency of photo-electrode with Paste A+B is slightly reduced when scattering layer (Paste C) is added, due to the thickness of the layers exceeding the optimum value.

As discussed in Section 3.3, double layer Paste A, having higher dye loading than that of Paste A+B, supposedly yields higher efficiency but our result shows otherwise. This is due to the haze effect of Paste B, where higher haze contributes to higher diffused transmittance [4].

The conversion efficiency improves when a dual titanium tetrachloride, ($TiCl_4$) treatment is applied to the DSSC (Table 3). The reasons for this are that the first $TiCl_4$ treatment is able to reduce recombination and improve adhesion between the TiO_2 and FTO glass substrate, whilst the second treatment increases the surface roughness factor of the TiO_2 in order to promote a higher amount of dye uptake and therefore increase J_{sc} [9].

Pore sizes in semiconductor layers can also affect performance of the DSSC. Table 4 shows the pore sizes of Paste A and Paste B. Mesoporous TiO_2 with suitable pore sizes makes the most of its high surface area and thereby allows a high uptake of dye to enhance the current density [12]. In our study, Paste A+B with suitable pore size recorded the highest conversion efficiency.

4. Conclusion

TiO_2 film thickness and roughness affect the performance of DSSC. As the film thickness is increased, the dye adsorption capability is increased. However, the film tends to crack when the TiO_2 film layer thickness has exceeded an optimum value. Our results show that TiO_2 paste with smaller particle sizes has higher adherence of dye molecules. In addition, layers with suitable pore sizes promote high uptake of dye. The addition of a scattering layer and/or $TiCl_4$ treatment also improves the performance of DSSC.

Acknowledgements

We thank the Ministry of Science, Technology and Innovation Malaysia (MOSTI) for financial support via ERGS Grant and UTAR Research Fund.

References

[1] B. O'Regan, M. Gratzel, A low-cost, high-efficiency solar cell based on dye-sensitized colloidal TiO_2 films, Nature 335 (1991) 737–740.

[2] M. Grätzel, Photoelectrochemical cells, Nature 414 (2001) 338–344.

[3] A. Hagfeldt, M. Gratzel, Molecular photovoltaics, Accounts of Chemical Research 33 (2000) 269–277.

[4] Y. Chiba, A. Islam, Y. Watanabe, R. Komiya, N. Koide, L. Han, Dye-sensitized solar cells with conversion efficiency of 11.1%, Japanese Journal of Applied Physics 45 (2006) L638–L640.

[5] F. Gao, Y. Wang, D. Shi., J. Zhang, M. Wang, X. Jing, R. Humphry-Baker, P. Wang, S.M. Zakeeruddin, M. Gratzel, Enhance the optical absorptivity of nanocrystalline TiO_2 film with high molar extinction coefficient ruthenium sensitizers for high performance dye-sensitized solar cells, Journal of the American Chemical Society 130 (2008) 10720–10728.

[6] J.K. Lee, B.H. Jeong, S.I. Jang, Y.W. Jang, S.B. Lee, M.R. Kim, Preparation of TiO_2 pastes and its application to light-scattering layer for dye-sensitized solar cell, Industrial and Engineering Chemistry Research 15 (2009) 724–729.

[7] N.G. Park, K. Kim, Transparent solar cells based on dye-sensitized nanocrystalline semiconductors, Physica Status Solidi A 205 (2008) 1895–1904.

[8] R. Katoh, N. Fuke, A. Furube, N. Koide, Effect of dye coverage on photo-induced electron injection efficiency in N719-sensitized nanocrystalline TiO_2 films, Chemical Physics Letters 489 (2010) 202–206.

[9] S. Ito, T.N. Murakami, P. Comte, P. Liska, C. Grätzel, M.K. Nazeeruddin, M. Gratzel, Fabrication of thin film dye sensitized solar cells with solar to electric power efficiency over 10%, Thin Solid Film 516 (2008) 4613–4619.

[10] D.J. Yang, Hun Park, S.J. Cho, H.G. Kim, W.Y. Choi, TiO_2-nanotube-based dye-sensitized solar cells fabricated by an efficient anodic oxidation for high surface area, Journal of Physics and Chemistry of Solids 69 (2008) 1272–1275.

[11] S. Ito, T. Kitamura, Y. Wada, S. Yanagida, Facile fabrication of mesoporous TiO_2 electrodes for dye solar cells: chemical modification and repetitive coating, Solar Energy Materials and Solar Cells 76 (2003) 3–13.

[12] T.K. Yun, S.S. Park, D. Kim, Y.K. Hwang, S. Huh, J.Y. Bae, Y.S. Won, Pore-size effect on photovoltaic performance of dye-sensitized solar cells composed of mesoporous anatase-titania, Journal of Power Sources 196 (2011) 3678–3682.